Estimation Formulas for the Specific Absorption Rate in Humans Exposed to Base-Station Antennas

Marie-Christine Gosselin, Günter Vermeeren, Sven Kühn, Valpré Kellerman, Stefan Benkler, Tero M. I. Uusitupa, Wout Joseph, *Member, IEEE*, Azeddine Gati, *Member, IEEE*, Joe Wiart, Frans J. C. Meyer, Luc Martens, *Member, IEEE*, Toshio Nojima, Takashi Hikage, Quirino Balzano, *Life Fellow, IEEE*, Andreas Christ, and Niels Kuster, *Fellow, IEEE*

***Abstract*—The demonstration of compliance with guidelines for human exposure to base-station antennas can be a time consuming process or often results in overly conservative estimates. To alleviate this burden and reduce the overestimation, approximation formulas for the whole-body average specific absorption rate (SAR) and the peak spatial SAR of human bodies using readily available basic antenna parameters have been developed and validated in this study. The formulas can be used for adults standing in the radiating near field of base-station antennas operating between 300 MHz and 5 GHz, at distances larger than 200 mm. It is shown that the 95th-percentile absorption for the human population can be well approximated by the absorption mechanism and statistical data of weight, height, and body-mass index of the human population. The validation was performed numerically using three anatomical human models (Duke, Ella, and Thelonious) exposed to 12 generic base-station antennas in the frequency range 300 MHz to 5 GHz at six distances between 10 mm and 3 m. From the 432 evaluated configurations, the estimation formulas for adult models are proven to be conservative in predicting the SAR exposure values of the two adults, but as expected not of the child.**

***Index Terms*—Anatomical models, base-station antennas, electromagnetic fields, occupational exposure, safety limits, specific absorption rate (SAR).**

Manuscript received October 8, 2009; revised August 17, 2010 and November 24, 2010; accepted February 13, 2011. Date of publication June 9, 2011; date of current version November 18, 2011. This work was supported by the Mobile Manufacturers Forum and the Global System for Mobile Communication Association.

M.-C. Gosselin, S. Kühn, A. Christ, and N. Kuster are with the Foundation for Research on Information Technologies in Society (IT'IS), Zurich 8048, Switzerland (e-mail: gosselin@itis.ethz.ch; kuehn@itis.ethz.ch; christ@itis.ethz.ch; kuster@itis.ethz.ch).

G. Vermeeren, W. Joseph, and L. Martens are with the Department of Information Technology (INTEC), Ghent University, Ghent 9000, Belgium (e-mail: gunter.vermeeren@intec.ugent.be; wout.joseph@intec.ugent.be; luc.martens@intec.ugent.be).

V. Kellerman and F. J. C. Meyer are with EM Software & Systems, Stellenbosch, Western Cape 7600, South Africa (e-mail: valpre@emss.co.za; fjcmeyer@emss.co.za).

S. Benkler is with Schmid and Partner Engineering AG, Zurich 8004, Switzerland (e-mail: benkler@speag.com).

T. M. I. Uusitupa is with Aalto University School of Science and Technology, Espoo 02150, Finland (e-mail: tero.uusitupa@aalto.fi).

A. Gati and J. Wiart are with France Telecom Research & Development, Paris 75018, France (e-mail: azeddine.gati@orange-ftgroup.com; joe.wiart@orange-ftgroup.com).

T. Nojima and T. Hikage are with Hokkaido University, Sapporo 060-0809, Japan (e-mail: nojima@ice.eng.hokudai.ac.jp; hikage@wtemc.ist.hokudai.ac.jp).

Q. Balzano is with the University of Maryland, College Park, MD 20742 USA (e-mail: qbalzano@umd.edu).

Digital Object Identifier 10.1109/TEMC.2011.2139216

I. Introduction

In MOST countries, exposure to RF fields from base-station antennas is regulated by the guidelines published by the International Commission on Non-Ionizing Radiation Protection (ICNIRP) [1] or by the rules from the Institute of Electrical and Electronics Engineers (IEEE) [2].

In [1], two different types of limits are defined: the basic restrictions, limiting the specific absorption rate (SAR) and the current density inside the body, and the reference levels, limiting the incident electric and magnetic fields. The latter are secondary and derived from the basic restriction limits. In the near field of radiating structures, e.g., close to base-station antennas, the reference levels can be very conservative, i.e., the ratio between incident field values and SAR is much larger than that of reference levels and basic restrictions. Therefore, measurements of the fields around base-station antennas lead to very conservative exposure estimates. On the other hand, on-site SAR measurements are technically challenging and laboratory measurements at large distances from RF sources are not always possible.

In the vicinity of base-station antennas, where the highest RF fields are present, the exposure scenarios are, however, relatively well defined. The data sheet of the antenna typically contains information about its dimensions and radiating properties. Thus, the development of an SAR estimation for humans standing in the radiative near field or far field of base-station antennas is desirable.

Exposure of anatomical human bodies to base-station antennas has already been studied in the past [3], [4], but the exposure matrices used were not extensive. Moreover, most studies involving simulation of detailed heterogeneous human models in front of base-station antennas have used the Visible Human model [5], [6]. This model has been found to be neither representative of the average human nor leading to worst case absorption. Plane-wave exposure of various human models shows that a compliant SAR for the Visible Human model does not necessarily lead to a compliant exposure of a smaller model [7] and that the guidelines are not always conservative for the exposure of children [7], [8].

Some work has been done in [9] to extract formulas to estimate the SAR due to exposure to base-station antennas. This estimation is based on a fit of a large set of SAR data extracted from the literature. However, it only includes a few adult models and the statistical evaluation is biased by the use of the Visible Human model. Moreover, the frequency range is limited to 800–2200 MHz.

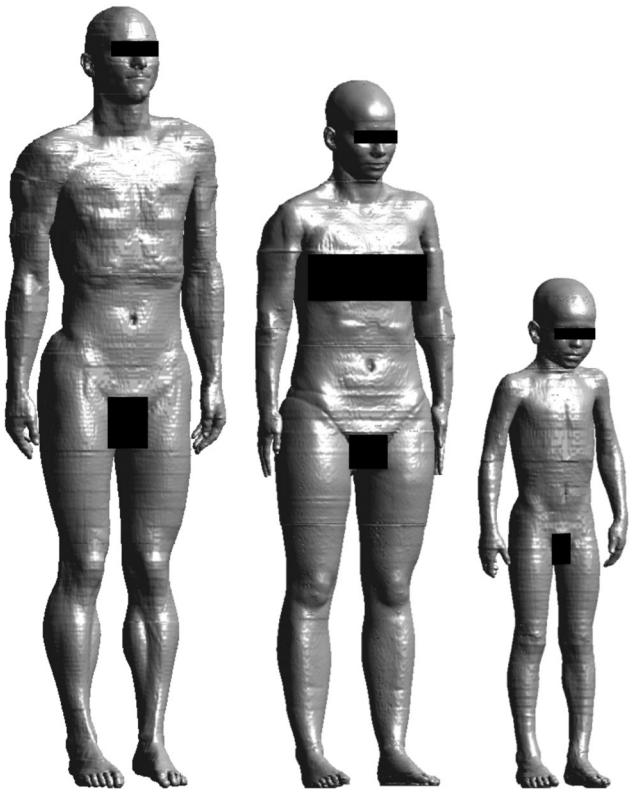

Fig. 1. Three anatomical human models from the VF. From left to right: VFM, VFF, and VFB.

A more general approach to this problem consists of applying physical considerations to develop estimation formulas and comparing the results from the obtained formulas with the SAR values from an extensive exposure matrix of humans in front of base-station antennas.

II. Objectives

The main objective of this study is to support the development of the International Electrotechnical Commission (IEC) standard PT62232. In detail, this includes the following:

1) development of estimation formulas for the whole-body, 1 g, and 10 g SAR based on physical considerations as well as numerical results;
2) validation of the formulas by numerical evaluation of the whole-body average SAR (wbSAR) and peak spatial SAR (psSAR) of high-resolution anatomical models exposed to several base-station antennas at various distances and sides of exposure.

III. Methods

A. Anatomical Body Models

As shown in Fig. 1, three members of the virtual family (VF) [10] were used: Duke, the virtual family male (VFM), Ella, the virtual family female (VFF), and Thelonious, the 6-year-old virtual family boy (VFB). These models, distinguishing about 80 tissue types, are based on medical resonance images (MRI) of healthy volunteers. The dielectric parameters of the tissues were assigned according to the parametric model described in [11] and to the equivalence table provided with the VF models. Table I presents the age, weight, height, cross-section surface S_{cs} and skin surface $S_{\mathrm{Du\ Bois}}$ given by (1), of the three models.

TABLE I
Characteristics of the Human Models

		VFM	VFF	VFB
Age		34	26	6
Weight	kg	72.2	58.1	19.4
Height	m	1.80	1.63	1.18
S_{cs}[a]	m^2	0.560	0.484	0.230
S_{DuBois}	m^2	1.91	1.62	0.805

[a] The cross-section, defined as the area of the projection of the body in a plane perpendicular to the direction of propagation of a plane wave, is given for exposure from the front or the back of the models.

The human models developed for the VF are representative of average humans in the population (based on statistical data from [12]). As the estimation formulas are developed based on the premise of being conservative for 95% of the adult population, it is not expected that the simulation results from the VF models exceed the exposure predicted by the estimation formulas.

B. Antennas

Twelve generic base-station antenna models were developed based on realistic antennas: two for each of six frequencies within the range 300 MHz to 5 GHz. The antennas were selected to represent typical wireless base-station antennas. Table II summarizes their specifications, including N, the number of elements, D, the largest dimension of the antenna, $\Phi_{3\mathrm{dB}}$, the horizontal half-power beamwidth (HPBW), and $\Theta_{3\mathrm{dB}}$, the vertical HPBW. The antenna models were validated by comparing their far-field characteristics, as well as the electric and magnetic fields in four planes at various distances in front of the antennas, from finite-difference time-domain (FDTD) method and method of moments (MoM) simulations to the values from the data sheet of the manufacturer.

C. Numerical Methods

All the numerical evaluations of the exposure of a human body in front of a base-station antenna were performed using the in-house simulation platform SEMCAD X (SPEAG, Switzerland), which includes a postprocessor for evaluation of the psSAR according to [13] for any user-specified averaging mass.

Placement of the models at great distances in terms of wavelength causes the computational problem to become very large when using the traditional FDTD method. A new method, called the generalized Huygens box (GHB) method [14], has been developed and implemented in SEMCAD X. In this method, the incident fields from the antenna are computed in free space using either FDTD, MoM, an analytical method, or some other method, and recorded on the surface of the GHB surrounding the human model. For the exposure evaluation, which requires a locally very fine grid resolution, the previously recorded fields are interpolated and enforced on the FDTD grid at the surface of the GHB [14] while the model is inside. The SAR computation is then performed as when using the traditional FDTD method. The GHB method was only used for configurations where the

TABLE II
SPECIFICATIONS OF THE GENERIC BASE-STATION ANTENNAS

Frequency MHz	Antenna	Polarization	N	Height mm	Width mm	D mm	Dir. dBi	$\Phi_{3\mathrm{dB}}$ degrees	$\Theta_{3\mathrm{dB}}$ degrees	Example of commercial model
300	300MHz H66V60	vertical	2	750	1000	1250	9	66	60	K 52 30 57
	300MHz H116V32	vertical	2	1530	420	1587	9	116	32	K 73 95 04
450	450MHz H118V35	vertical	2	1020	280	1058	9.3	118	35	K739504
	450MHz H188V19	vertical	4	1960	140	1965	10	188	19	DAPA 1280
900	900MHz H65V7	45°	8	2562	302	2580	18.5	65	7	K739 624
	900MHz H90V9	vertical	6	1922	242	1937	15.9	90	9	K736 863
2100	2100MHz H66V7	45°	10	1302	132	1309	19.25	66	7	K742 212
	2100MHz H90V81	vertical	1	204	164	262	8.1	90	81	K742 149
3500	3500MHz H20V19	vertical	4×4	245	245	346	20	20	19	Alvarion
	3500MHz H65V9	vertical	12	482	62	486	17.3	65	9	Alvarion
5000	5000MHz H66V35	vertical	4	81	41	91	11.8	66	35	Huber & Suhner
	5000MHz H360V8	vertical	6	330	0.5	330	10.5	360	8	SMCANT-00M10

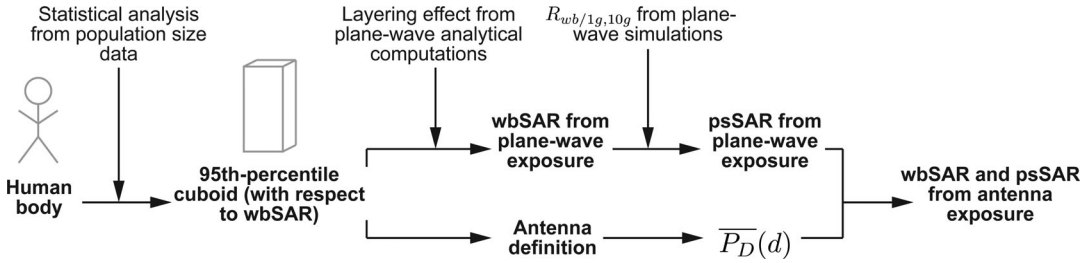

Fig. 2. Diagram representing the steps in elaborating the SAR estimation formulas.

coupling between the human model and the antenna could be neglected.

IV. ESTIMATION FORMULAS

The following section describes the steps in the elaboration of the estimation formulas of the wbSAR and psSAR for exposure from base-station antennas. A diagram of these steps is presented in Fig. 2. First, the exposed human body is represented by a cuboid, as already proposed in [15] and [16], but never used before with the aim of developing any kind of analytical estimation. An analysis of the population statistical distribution of weight, height, and body-mass index (bmi) allows us to derive the dimensions of a human body leading to a conservative exposure for 95% of the population. A simple expression of the wbSAR is found and validated for plane-wave exposure, including enhancement due to tissue layers. An analysis of plane-wave results is then performed to derive worst case ratios of wbSAR on psSAR.

The expression of the average power density along a vertical line in the boresight direction of the antenna is taken from [17]. Knowing that exposure from a base-station antenna is not uniform over the entire cross section of the body, an effective radiated surface of the exposed cuboid is defined. Thereafter, the formulas of the wbSAR and psSAR are determined, depending on readily available antenna parameters, the radiated power, the antenna-cuboid distance, and the dimensions of the 95th-percentile human.

A. Generic Human Model

As a first step, the human phantom is approximated by a cuboid with the same height, weight, and skin surface as the human it represents. The cuboid is homogeneous with a density $\rho = 1000$ kg/m^3. The skin surface of a human S can, for example, be approximated from its weight m and its height H by DuBois and DuBois [18]

$$S_{\mathrm{DuBois}}[\mathrm{cm}^2] = 71.84(m[\mathrm{kg}])^{0.425}(H[\mathrm{cm}])^{0.725}. \quad (1)$$

The total surface of the cuboid is calculated using (1) and its volume is found from its weight and density. The surface area and the volume V can also be expressed as a function of the dimensions of the cuboid: its height H, width W, and depth D. The latter two are found by solving this system of equations of S and V. The largest of the two obtained dimensions is associated with the width and the smallest with the depth, which maximizes the cross section for frontal exposure and leads to a unique cuboid for each considered body. The dielectric properties of the homogeneous cuboid are set according to [19].

B. 95th-Percentile Representative Phantom

Instead of generating the cuboid from the dimensions of a specific human body, a more general approach of the estimation formulas consists of using the dimensions of a realistic human body that would lead to a worst case exposure covering 95% of the adult human population. The highest wbSAR is reached for a maximum ratio of S_{cs}/m [3], [7]. For a uniform exposure over the entire cross section of the cuboid, the wbSAR, $\mathrm{SAR}_{\mathrm{wb}}$, can be estimated by

$$\mathrm{SAR}_{\mathrm{wb}} = \frac{S_{\mathrm{cs}}}{m} P_{D,t} \quad (2)$$

where $P_{D,t}$ is the power density transmitted into the solid and $S_{\mathrm{cs}} = W \cdot H$ is taken as the frontal surface of the cuboid, as

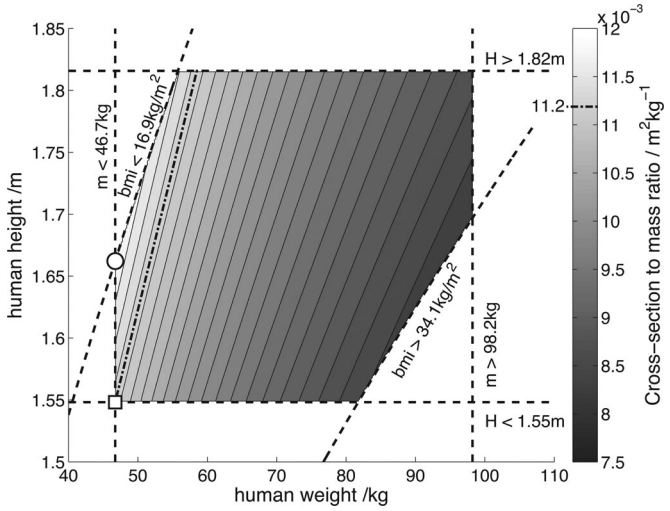

Fig. 3. Cross section to mass ratio of the associated cuboid as a function of the weight and height of the human body. Only the points for which the weight, the height, and the bmi are within the range "mean $\pm$ 2 $\times$ standard deviation" are displayed, i.e., $46.7\,\text{kg} < m < 98.2\,\text{kg}$, $1.55\,\text{m} < H < 1.82\,\text{m}$, and $16.9\,\text{kg/m}^2 < \text{bmi} < 34.1\,\text{kg/m}^2$, respectively.

it has been shown that frontal exposure leads to the highest wbSAR when exposed either to plane waves [7], [20] or to base-station antennas [3], [5].

Diverse Populations Collaborative Group [12] provides anthropometric data (mean and standard deviation of weight, height, and bmi) for several groups of adults from the U.S., Europe, and Asia. Assuming that these data are representative of the global population, 95% of the population have their weight, height, and bmi included in the range "mean $\pm$ 2 $\times$ standard deviation." Fig. 3 shows the cross section to mass ratio of cuboids based on weights, heights, and bmi within the range containing 95% of the population. The highest cross section to mass ratio of $12.0 \times 10^{-3}\,\text{m}^2/\text{kg}$, indicated by a circle in Fig. 3, is obtained for the lightest human and a maximum height, which is limited by the minimum bmi.

Under base-station antenna exposure, however, the entire body is typically not uniformly exposed; the power density is higher around the vertical center of the antenna. In this case, a shorter and wider human body would absorb more radiation. The shortest and lightest human, shown by a square in Fig. 3, leads to a cross section on the mass ratio of $11.2 \times 10^{-3}\,\text{m}^2/\text{kg}$. In the case of exposure to base-station antennas, this is more likely to lead to the highest wbSAR; thus, these dimensions were chosen to represent the 95th-percentile human (see Table III). For a typical base-station exposure, i.e., stronger in the center, the estimation will be conservative for 95% of the adults in the population. If, however, the base-station antenna is such that the exposure is uniform over the entire height of the model, we expect this cuboid to lead to a conservative estimation of the exposure for 90% of the adults: the chosen value of cross section on the mass ratio (square marker) is 94% of the maximum value (circle marker), itself leading to a 95% estimation.

TABLE III
DIMENSIONS OF THE CUBOID REPRESENTING THE 95TH-PERCENTILE HUMAN BODY

		95th-percentile cuboid
Weight	kg	46.7
Height	m	1.54
Width	m	0.339
Depth	m	0.089
S_{cs}	m^2	0.522
S_{DuBois}	m^2	1.40

C. Induced Power Density

The SAR is defined as a function of the electric field in a solid $E_{\text{rms},t}$

$$\text{SAR} = \frac{\sigma\,|E_{\text{rms},t}|^2}{\rho} \tag{3}$$

where σ and ρ are the conductivity and density of the material, respectively. On the other hand, one can use the properties of a base-station antenna to compute the power density averaged along a vertical line having the same height as the antenna (see Section IV-A). In the next paragraphs, the relationship between the transmitted electric field and the incident power density will be developed and used to express the SAR as a function of a quantity related to base-station antenna exposure: the incoming power density $P_{D,i}$.

The power density of an electromagnetic wave P_D is defined from its electric and magnetic fields E and H, respectively

$$\vec{P}_D = \Re\{\vec{E}_{\text{rms}} \times \vec{H}^*_{\text{rms}}\}. \tag{4}$$

Assuming plane-wave propagation, the electric and magnetic fields are orthogonal and the impedance of the wave is defined as $Z = E/H = \sqrt{\mu/\epsilon}$, where μ is the complex permeability and ϵ the complex permittivity.

For a plane wave coming from free space at normal incidence to a nonmagnetic medium of relative complex permittivity ϵ_r, the transmitted electric field E_t is related to the incident electric field E_i via the transmission coefficient $t = \frac{2}{1+\sqrt{\epsilon_r}}$. Using these definitions, the transmitted power density $P_{D,t}$ can be expressed as

$$P_{D,t} = Z_i\,|t|^2\,\Re\left\{\frac{1}{Z_t^*}\right\}P_{D,i} \tag{5}$$

where Z_i and Z_t are the impedance in the incidence and transmission media, respectively. And the transmitted electric field can be written as

$$|E_{\text{rms},t}|^2 = Z_i\,|t|^2\,P_{D,i}. \tag{6}$$

Using the SAR definition from (3), one can find the SAR at $x = 0$ inside a medium, $\text{SAR}(0)$, using (6), if the incident face of the medium is perpendicular to the direction of propagation of the incident wave

$$\text{SAR}(0) = \frac{\sigma}{\rho} Z_i\,|t|^2\,P_{D,i}(0). \tag{7}$$

D. Whole-body Average SAR

This section presents a general expression for the wbSAR, based on the same type of development as used in [21] for the 10 g psSAR, i.e., from an approximation based on the SAR at the surface of the model.

The average wbSAR, $\mathrm{SAR}_{\mathrm{wb}}$, is defined as the ratio of the total absorbed power to the total absorbing mass. In the case of a homogeneous solid, the average over the total volume V_{tot} can be written as a function of the position-dependant local SAR, $\mathrm{SAR}(x,y,z)$:

$$\mathrm{SAR}_{\mathrm{wb}} = \frac{1}{V_{\mathrm{tot}}} \iiint_{\mathrm{vol}} \mathrm{SAR}(x,y,z)dxdydz. \tag{8}$$

This expression is valid for a homogeneous solid of arbitrary shape, but the integral becomes much simpler to evaluate in the case of a cuboid. The edge effects and the reflections from the back of the cuboid are neglected, i.e., the cuboid is treated as a portion of half-space. For a wave propagating in the x-direction, we assume that the SAR in the yz-plane is uniform[1] over the "exposed region" R_{yz} and zero outside. The SAR decays exponentially along x from the surface of the medium to its depth x_d, so (8) becomes

$$\mathrm{SAR}_{\mathrm{wb}} = \frac{1}{V_{\mathrm{tot}}} \iiint_{\mathrm{vol}} \mathrm{SAR}(x)dxdydz \tag{9}$$

$$= \frac{1}{V_{\mathrm{tot}}} \iint_{R_{yz}} dydz \int_0^{x_d} \mathrm{SAR}(0) e^{\frac{-2x}{\delta}} dx \tag{10}$$

where δ is the penetration depth. Worst case will be reached for a thick model that will absorb all the power ($x_d \gg \delta$)

$$\mathrm{SAR}_{\mathrm{wb}} = \frac{1}{V_{\mathrm{tot}}} \frac{\delta}{2} \mathrm{SAR}(0) \iint_{R_{yz}} dydz. \tag{11}$$

For plane waves, the penetration depth is expressed as a function of the angular frequency ω, the real part of the relative permittivity ϵ_r', and the conductivity σ [22]

$$\delta = \frac{1}{\omega} \left[\left(\frac{\mu_0 \epsilon_r' \epsilon_0}{2} \right) \left(\sqrt{1 + \left(\frac{\sigma}{\omega \epsilon_r' \epsilon_0} \right)^2} - 1 \right) \right]^{-1/2}. \tag{12}$$

E. Tissue Layering

The enhancement of the SAR due to a layered structure compared to a homogeneous one has been shown exhaustively in the past [23]–[25]. In particular, the authors of [26] used far-field-like exposure, a simplified 1-D model of tissue–layer compositions, and a set of all the possible layer compositions at any location at the surface of any human body in the population. They have shown that the effect on the 10 g psSAR could be up to 3 dB.

Using the same set of layer compositions, computation model, and exposure, we have assessed the enhancement on the absorbed power integrated along the depth of the body, assuming that no reflections are coming from the back surface of the structure. We exposed the half-space layers of tissues to incident plane waves at seven different frequencies between 30 MHz and 5.8 GHz. The absorbed power in these structures was compared to the absorbed power in the homogeneous body with dielectric properties set according to [19].

Fig. 4. CDF of the enhancement of the absorbed power in a layered volume compared to a homogeneous volume [19] exposed to plane waves.

Fig. 4 shows the cumulative distribution function (CDF) of the enhancement of the total absorbed power in the different configurations of layers compared to a homogeneous solid. The configurations of layers causing the worst case enhancement (3 dB) are not found in every human body. Considering a realistic scenario where these configurations are present, it would be unreasonable to assume that they cover the entire cross section. So even if these configurations are present, the increase of the whole-body SAR would be lower than 3 dB. Furthermore, most of the configurations leading to enhancements higher than 2.5 dB include a thick layer of fat, which is inconsistent with the cuboid chosen in Section IV-B representing a thin human body. To avoid this overestimation, a more reasonable enhancement factor of 2.5 dB was chosen. The wbSAR including the layer enhancement factor will be a factor $10^{2.5/10}$ higher than the wbSAR of a homogeneous volume. This value is validated using plane-wave simulations in Section IV-F.

F. Whole-body Average SAR—Plane-Wave Exposure

For a cuboid exposed to uniform plane waves, the exposed region R_{yz} is simply the area of the surface of incidence S_{cs} and (11) becomes

$$\mathrm{SAR}_{\mathrm{wb}} = \frac{1}{V_{\mathrm{tot}}} \frac{\delta}{2} W_{\mathrm{body}} H_{\mathrm{body}} \mathrm{SAR}(0) \tag{13}$$

$$= \frac{\delta}{2D_{\mathrm{body}}} \mathrm{SAR}(0) \tag{14}$$

where D_{body}, W_{body}, and H_{body} are the depth, width, and height of the cuboid, respectively.

[1]For exposure from base-station antennas, the evaluation of the power density from the properties of the antenna is averaged over the height of the antenna (see Section IV-I).

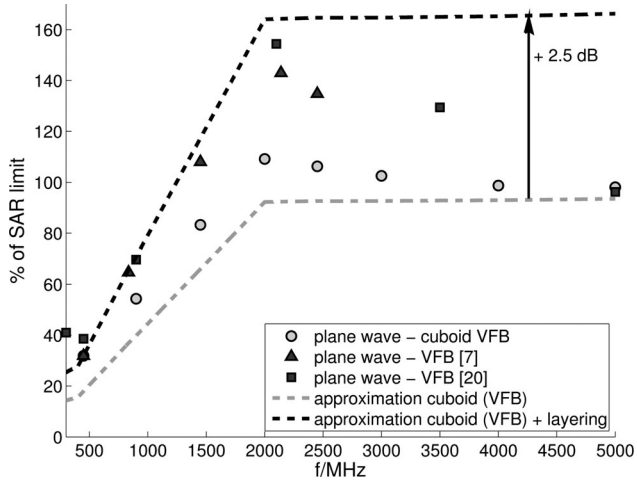

Fig. 5. Comparison between wbSAR of the heterogeneous VFB from plane-wave exposure [7], [20] and the cuboid approximation, for a power density exposure at ICNIRP level.

TABLE IV
ICNIRP [1] (10 kHz to 10 GHz) and IEEE [2] (300 kHz to 100 GHz) Basic Restrictions for Occupational Exposure

	source	SAR W/kg
Whole-body average	ICNIRP/IEEE	0.4
10 g in head and trunk	ICNIRP	10
10 g in limbs	ICNIRP	20
1 g in body[a]	IEEE	8

[a] The IEEE states that the 1 g limit is applicable to the entire body, except the hands, wrists, feet, and ankles, which should not exceed a 10 g psSAR of 20 W/kg (same value as the one from ICNIRP for the limbs).

To validate the cuboid approach and the layer enhancement factor of 2.5 dB, simulation results of plane waves were compared to the estimation of the wbSAR from (14) and (7). Fig. 5 shows the results from plane-wave exposure (worst case of polarization and exposure side) of the VFB from [7] and [20] between 300 MHz and 5 GHz. The results are expressed as the percentage of the wbSAR basic restriction reached for a plane-wave exposure at the reference level (according to ICNIRP, see Tables IV and V). Additional simulations were performed using a homogeneous cuboid based on the height and weight of the VFB (cuboid: 19.4 kg, 0.065 m $\times$ 0.253 m $\times$ 1.176 m) frontally exposed to vertically polarized plane waves. The dielectric properties were set according to [19], which are based on a 95% requirement for near-field exposure. The compensation factors introduced in [19] were not taken into account, since the enhancement due to tissue layering was considered separately here. Fig. 5 shows that the simulation of the cuboid (gray markers) as well as the estimation of the wbSAR based on its dimensions (gray line) is much lower than the wbSAR of the VFB (black markers) over the entire frequency range. The estimation based only on homogeneous considerations (gray line) is close to the simulation results of wbSAR of the homogeneous cuboid. On the other hand, the estimation including the layering enhancement of 2.5 dB (black line) is at the same level as the results of the VFB.

TABLE V
ICNIRP Reference Levels for Occupational Exposure

Frequency range	plane-wave power density $\mathrm{W/m^2}$
10-400 MHz	10
400-2000 MHz	$f/40$
2-300 GHz	50

For frequencies higher than 2 GHz, the dielectric properties from [19] lead to more conservative results from the cuboid simulations, as well as from the approximation including the layering enhancement. We can conclude that (14) and (7) combined with a layering enhancement factor of 2.5 dB are a good approximation for frequencies between 300 and 2000 MHz, and more conservative than the plane-wave simulation results for higher frequencies.

G. Peak Spatial SAR

The psSAR is highly dependent on the anatomical properties and posture of the phantom [20]. The position of the potential local enhancement parts of the body, typically the wrists, ankles, nose, or groin, relative to the local field maxima also has a direct influence on the psSAR value. Thus, the psSAR for a specific configuration of antenna and phantom is hard to evaluate without a simulation. However, the ratio between the wbSAR and the psSAR determined from plane-wave simulations allows a rough but simple worst case estimation. Fig. 6 uses plane-wave exposure data of standing models from [7] and [20] to show $R_{\mathrm{wb}}/R_{1\mathrm{g},10\mathrm{g}}$, the ratio between the wbSAR (to its ICNIRP basic restriction: $R_{\mathrm{wb}} = \mathrm{SAR}_{\mathrm{wb}}/\mathrm{SAR}_{\mathrm{wb}}^{\mathrm{limit}}$) and the psSAR (to its ICNIRP basic restriction: $R_{10\mathrm{g}} = \mathrm{SAR}_{10\mathrm{g}}/\mathrm{SAR}_{10\mathrm{g}}^{\mathrm{limit}}$ or $R_{1\mathrm{g}} = \mathrm{SAR}_{1\mathrm{g}}/\mathrm{SAR}_{1\mathrm{g}}^{\mathrm{limit}}$).

A ratio depending on the frequency range is used to estimate the psSAR from the estimation of the wbSAR

$$R_{\mathrm{wb}/1\mathrm{g}} = \begin{cases} 0.6 & \text{if } 300\ \mathrm{MHz} \le f \le 2.5\ \mathrm{GHz} \\ 0.3 & \text{if } 2.5\ \mathrm{GHz} < f \le 5\ \mathrm{GHz} \end{cases} \quad (15)$$

$$R_{\mathrm{wb}/10\mathrm{g}} = \begin{cases} 1.5 & \text{if } 300\ \mathrm{MHz} \le f \le 2.5\ \mathrm{GHz} \\ 1 & \text{if } 2.5\ \mathrm{GHz} < f \le 5\ \mathrm{GHz}. \end{cases} \quad (16)$$

This frequency-dependent ratio is based on plane-wave exposure of standing models. Since it does not consider the eventual local enhancements due to the radiation pattern of the antenna or the posture of the model, it should at least be conservative enough to include all the results of plane-wave exposure presented here. Other postures might cause substantially higher psSAR, as shown in [20].

The expression of the psSAR ($\mathrm{SAR}_{1\mathrm{g}}$ or $\mathrm{SAR}_{10\mathrm{g}}$) based on these ratios and on (14) for wbSAR is

$$\frac{\mathrm{SAR}_{1\mathrm{g},10\mathrm{g}}}{\mathrm{SAR}_{1\mathrm{g},10\mathrm{g}}^{\mathrm{limit}}} = \frac{1}{R_{\mathrm{wb}/1\mathrm{g},10\mathrm{g}}} \frac{\mathrm{SAR}_{\mathrm{wb}}}{\mathrm{SAR}_{\mathrm{wb}}^{\mathrm{limit}}} \quad (17)$$

$$\mathrm{SAR}_{1\mathrm{g},10\mathrm{g}} = \frac{1}{2R_{\mathrm{wb}/1\mathrm{g},10\mathrm{g}}} \frac{\mathrm{SAR}_{1\mathrm{g},10\mathrm{g}}^{\mathrm{limit}}}{\mathrm{SAR}_{\mathrm{wb}}^{\mathrm{limit}}} \frac{\delta}{D_{\mathrm{body}}} \mathrm{SAR}(0). \quad (18)$$

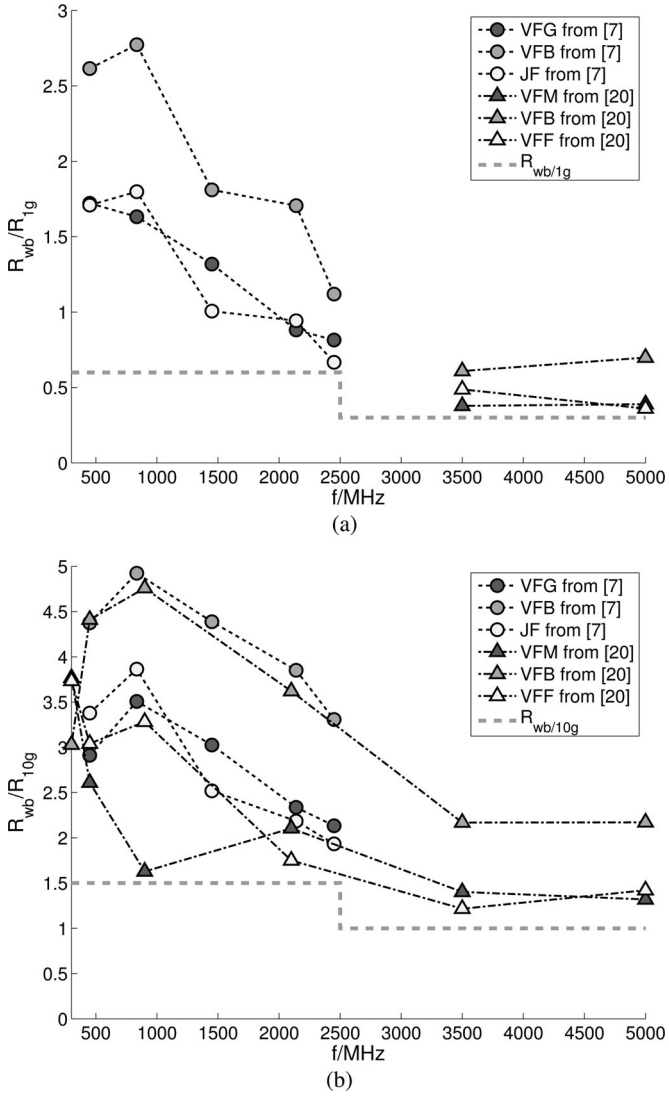

Fig. 6. Ratio of the wbSAR to the psSAR for standing models under plane-wave exposure from [7] and [20]. The curves of $R_{\mathrm{wb/1g}}$ (15) and $R_{\mathrm{wb/10g}}$ (16) are also represented. (a) $R_{\mathrm{wb}}/R_{\mathrm{1g}}$, (b) $R_{\mathrm{wb}}/R_{\mathrm{10g}}$.

H. Cylindrical Propagation—Radiating Near Field

It was shown in [17] that cylindrical propagation could be assumed in the radiating near field of a collinear array antenna. The power flux is then confined within the horizontal HPBW Φ_{3dB} and the overall height of the antenna L. The average power density[2] $\overline{P_D}$ along a vertical line of length L at a distance r from the center of phase of the antenna in the boresight direction is given by

$$\overline{P_D}(r,\Phi_{\mathrm{3dB}}) = \frac{P_{\mathrm{rad}}}{\Phi_{\mathrm{3dB}} r L \sqrt{1+\left(\frac{r}{r_0}\right)^2}}$$

$$r_0 = \frac{\Phi_{\mathrm{3dB}}}{4\pi} G_A L \tag{19}$$

[2]It has previously been mentioned by our group [3] that (19) comes from [27], but as was pointed out to us by Dr. Faraone, that was a misinterpretation, and (19) comes from [17]. This does not influence any of the statements made in [3].

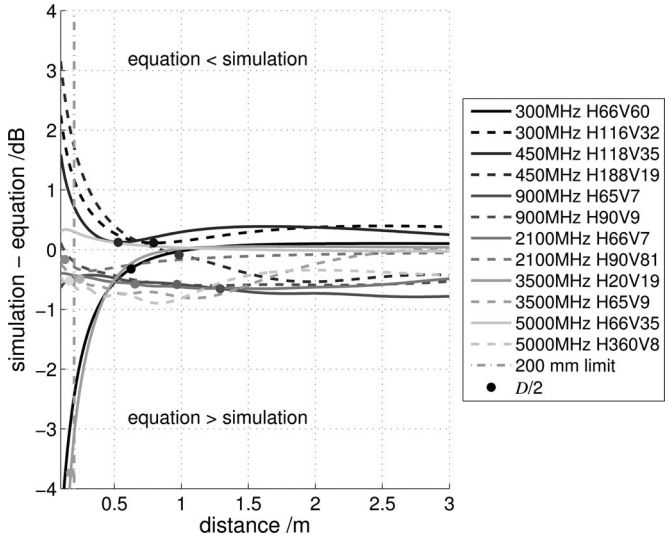

Fig. 7. Comparison of average power density from simulations and calculated from (19). For each antenna, the $D/2$ limit is shown by a point on the curve.

where P_{rad} is the power radiated from the antenna and G_A its directivity.

Equation (19) and the physical characteristics of the antennas were used to compute the average power density along a vertical line parallel to the axis of the 12 antennas described in Section III-B. Fig. 7 compares the results of (19) with the computation of the average power density from free-space simulations.

Equation (19) should be used with caution at small distances from very large antennas (where $D/2 > 200\,\mathrm{mm}$, such as the 300-, 450-, and 900-MHz antennas in Fig. 7) as well as with antennas for which the width is comparable to the height (such as the 300 MHz H66V60 and the 3500 MHz H20V19) since (19) is based on the hypothesis that the antenna has a slender shape. However, for the 12 antennas used in this paper and for distances larger than 500 mm, the equation either underestimates the simulation results by no more than to 0.4 dB or overestimates them, leading to a more conservative SAR estimation, by at most 0.8 dB. Fig. 7 shows that (19) is also a good approximation in the far field of the antennas.

I. Whole-body Average SAR—Base-Station Antennas

In (11), the exposed region R_{yz} depends strongly on the human model in front of the antenna and the characteristics of the antenna itself. Once again, a simple case is to approximate the human body by a cuboid of depth D_{body}, width W_{body}, and height H_{body}. However, the entire height or width of its cross section might not be homogeneously exposed by the wave coming from the antenna. The exposed portion of its width and height are named W_{eff} and H_{eff}, respectively. In this case, (11) for the wbSAR can be written as

$$\mathrm{SAR_{wb}} = \frac{1}{V_{\mathrm{tot}}} \frac{\delta}{2} W_{\mathrm{eff}} H_{\mathrm{eff}} \mathrm{SAR}(0) \tag{20}$$

$$= \frac{1}{2} \frac{\delta}{D_{\mathrm{body}}} \frac{W_{\mathrm{eff}}}{W_{\mathrm{body}}} \frac{H_{\mathrm{eff}}}{H_{\mathrm{body}}} \mathrm{SAR}(0). \tag{21}$$

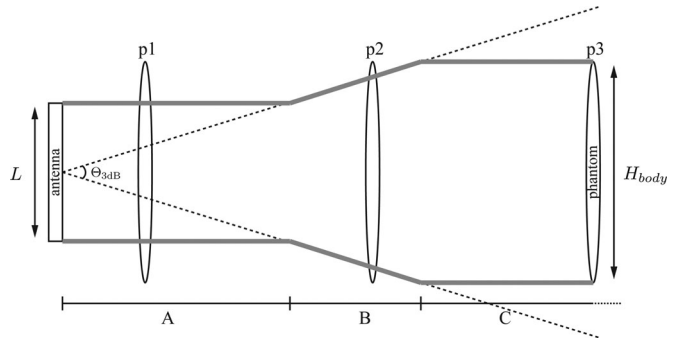

Fig. 8. Schematic side view of the exposed vertical length as defined in (23), at various distances from the antenna, depending on its vertical opening angle. The bold lines indicate the upper and lower boundaries of H_{eff}.

We consider that the model is exposed over its entire width ($W_{\text{eff}} = W_{\text{body}}$), which is a worst case assumption. However, we assume that the exposed portion of its height varies with the distance between the body and the antenna, the height of the phantom, and the beam spread H_{beam}, calculated from the far-field characteristics of the antenna (vertical HPBW, $\Theta_{3\text{dB}}$)

$$H_{\text{beam}} = 2d\tan(\Theta_{3\text{dB}}/2) \tag{22}$$

where d is the distance between the outer most point of the antenna and a box bounding the human model. The expression of H_{eff} chosen is shown in (23) and represented in Fig. 8

$$H_{\text{eff}} = \begin{cases} H_{\text{body}} & \text{if } H_{\text{body}} \le L \\ \text{else} & \\ L & \text{if } H_{\text{beam}} < L, H_{\text{body}} \quad \text{(A)} \\ H_{\text{beam}} & \text{if } L \le H_{\text{beam}} < H_{\text{body}} \quad \text{(B)} \\ H_{\text{body}} & \text{if } H_{\text{body}} \le H_{\text{beam}} \quad \text{(C)}. \end{cases} \tag{23}$$

If the phantom is shorter than the antenna, H_{eff} is equal to H_{body}, regardless of the antenna-body distance. Otherwise, if the phantom is taller than the antenna and the beam spread (see Fig. 8, position p1), H_{eff} is equal to the height of the antenna. If the beam spread is bigger than the antenna height, but still shorter than the phantom (see Fig. 8, position p2), the height of the beam spread is taken for H_{eff}. And if the phantom is shorter than the beam spread, the entire height of the body is exposed (see Fig. 8, position p3), so H_{eff} is equal to H_{body}. Vertically and horizontally, the center of the human body is considered to be aligned with the center of the antenna, which maximizes the exposed height and width (trunk), thus leading to worst case exposure.

J. Issues Relative to Short Antenna-Body Distances

For short antenna-human body distances, the complex shape of the human body leads to a high uncertainty of the distance. Moreover, the assumptions made in the last paragraphs are no longer valid very close to the antenna ($d < \lambda/2\pi$). The field is complex and no general equation can easily be assumed or derived. The energy reflected by the human can possibly be very strong, changing the impedance of the sources and, thus, the radiating properties of the antenna [26]. In Refs. [28] and [29], measurements for distances up to 200 mm from the antenna are suggested. We also propose that dosimetric measurements be made closer than 200 mm to ensure compliance with the guidelines.

K. Final Form of the Estimation Formulas

This section presents the final version of the estimation formulas in their general form, with[3] $r \simeq d$. The frequency range has been restricted to the range within which we could validate the formulas with the simulation results (see Section V), i.e., 300 MHz to 5 GHz. The equations do not include possible effects produced by the presence of reflective walls or ground plane as studied in [30]

$$\text{SAR}_{\text{wb}} = \frac{10^{0.25}}{2}\frac{\delta}{D_{\text{body}}}\frac{W_{\text{eff}}}{W_{\text{body}}}\frac{H_{\text{eff}}}{H_{\text{body}}}\text{SAR}(0) \tag{24}$$

$$\text{SAR}_{1\text{g},10\text{g}} = \frac{10^{0.25}}{2R_{\text{wb}/1\text{g},10\text{g}}}\frac{\text{SAR}_{1\text{g},10\text{g}}^{\text{limit}}}{\text{SAR}_{\text{wb}}^{\text{limit}}}\frac{\delta}{D_{\text{body}}}\text{SAR}(0) \tag{25}$$

with

$$\text{SAR}(0) = \frac{\sigma Z_i\,|t|^2\,P_{\text{rad}}}{\rho\Phi_{3\text{dB}}Ld}\left[1+\left(\frac{4\pi d}{\Phi_{3\text{dB}}G_A L}\right)^2\right]^{-1/2} \tag{26}$$

$$R_{\text{wb}/1\text{g}} = \begin{cases} 0.6 & \text{if 300 MHz} \le f \le \text{2.5 GHz} \\ 0.3 & \text{if 2.5 GHz} < f \le \text{5 GHz} \end{cases} \tag{27}$$

$$R_{\text{wb}/10\text{g}} = \begin{cases} 1.5 & \text{if 300 MHz} \le f \le \text{2.5 GHz} \\ 1 & \text{if 2.5 GHz} < f \le \text{5 GHz} \end{cases} \tag{28}$$

$$H_{\text{eff}} = \begin{cases} H_{\text{body}} & \text{if H}_{\text{body}} \le L \\ \text{else} & \\ L & \text{if H}_{\text{beam}} < L, H_{\text{body}} \\ H_{\text{beam}} & \text{if } L \le H_{\text{beam}} < H_{\text{body}} \\ H_{\text{body}} & \text{if } H_{\text{body}} \le H_{\text{beam}} \end{cases} \tag{29}$$

$$H_{\text{beam}} = 2d\tan(\Theta_{3\text{dB}}/2) \tag{30}$$

$$W_{\text{eff}} = W_{\text{body}} \tag{31}$$

$$t = \frac{2}{1+\sqrt{\epsilon}} \tag{32}$$

$$\delta = \frac{1}{\omega}\left[\left(\frac{\mu_0\epsilon_r'\epsilon_0}{2}\right)\left(\sqrt{1+\left(\frac{\sigma}{\omega\epsilon_r'\epsilon_0}\right)^2}-1\right)\right]^{-1/2}. \tag{33}$$

L. Compact Form of the 95th-Percentile Estimation Formulas

The estimation formulas are written here in a more compact form based on the premise of covering 95% of the adult human

[3]The distance r used in (19) is measured from the center of phase of the antenna, which corresponds to the surface of the back reflector if one is present. On the other hand, d is defined as the distance between the outer most point of the antenna and a box enclosing the body. Taking $r \simeq d$ leads to an underestimation of r, so a higher power density, thus a higher SAR estimation. Antenna users can only measure the distance from the radome of a given antenna, so that the approximation $r \simeq d$ is both more representative of practical measurements and more conservative.

TABLE VI
PIECEWISE LINEAR APPROXIMATION OF $C(f)$[a]

f MHz	$C(f)$ $10^{-4}\,\mathrm{m}^3/\mathrm{kg}$
300	6.3
900 - 5000	8.1

[a] The approximation of $C(f)$ results in a deviation of less than 5%. For frequencies between 300 and 900 MHz, a linear interpolation should be used.

population. To simplify the expression of the estimation formulas, the parameters that present only a frequency dependence have been gathered into a separate parameter $C(f)$:

$$\mathrm{SAR}_{\mathrm{wb}} = C(f)\frac{H_{\mathrm{eff}}}{0.089\,\mathrm{m}\times 1.54\,\mathrm{m}}\frac{P_{\mathrm{rad}}}{\Phi_{3\mathrm{dB}}Ld} \times\left[1+\left(\frac{4\pi d}{\Phi_{3\mathrm{dB}}G_A L}\right)^2\right]^{-1/2} \tag{34}$$

$$\mathrm{SAR}_{1\mathrm{g},10\mathrm{g}} = 25\times\mathrm{SAR}_{\mathrm{wb}}\frac{1.54\,\mathrm{m}}{H_{\mathrm{eff}}}\frac{1}{R_{\mathrm{wb}/1\mathrm{g},10\mathrm{g}}} \tag{35}$$

$$H_{\mathrm{eff}} = \begin{cases} 1.54\mathrm{m} & \text{if } 1.54\,\mathrm{m}\le L \\ \text{else} & \\ L & \text{if } H_{\mathrm{beam}} < L, 1.54\,\mathrm{m} \\ H_{\mathrm{beam}} & \text{if } L\le H_{\mathrm{beam}} < 1.54\,\mathrm{m} \\ 1.54\,\mathrm{m} & \text{if } 1.54\,\mathrm{m}\le H_{\mathrm{beam}} \end{cases} \tag{36}$$

$$H_{\mathrm{beam}} = 2d\tan(\Theta_{3\mathrm{dB}}/2) \tag{37}$$

$$R_{\mathrm{wb}/1\mathrm{g}} = \begin{cases} 0.6 & \text{if 300 MHz} \le f \le \text{2.5 GHz} \\ 0.3 & \text{if 2.5 GHz} < f \le \text{5 GHz} \end{cases} \tag{38}$$

$$R_{\mathrm{wb}/10\mathrm{g}} = \begin{cases} 1.5 & \text{if 300 MHz} \le f \le \text{2.5 GHz} \\ 1 & \text{if 2.5 GHz} < f \le \text{5 GHz} \end{cases} \tag{39}$$

$$C(f) = \frac{10^{0.25}}{2}\delta(f)\,|t(f)|^2\,\frac{\sigma(f)}{\rho}\sqrt{\frac{\mu_0}{\epsilon_0}}. \tag{40}$$

The coefficient $C(f)$ is frequency dependent. It can be evaluated using the values of conductivity and permittivity from [19]. Table VI shows the approximation of $C(f)$. The deviation in $C(f)$ is less than 5%, which will lead to an error lower than 5% in the SAR.

V. NUMERICAL VALIDATION

The SAR in heterogeneous structures such as a human body is impossible to measure, even with state-of-the-art systems. The results of wbSAR and psSAR from the approximation formulas were, thus, validated by comparison to numerical results from the commercial FDTD simulation platform SEMCAD X using an extensive list of configurations of humans in front of base-station antennas. To further verify the simulation results, a few specific configurations were run independently by various groups using other simulation tools, such as the commercial platforms FEKO (EMSS, South Africa) and XFdtd (Remcom, PA), as well as the in-house codes from Hokkaido University, France Telecom Research and Development, and Aalto University. The extensive exposure matrix consists of all the possible combinations of the following specifications:

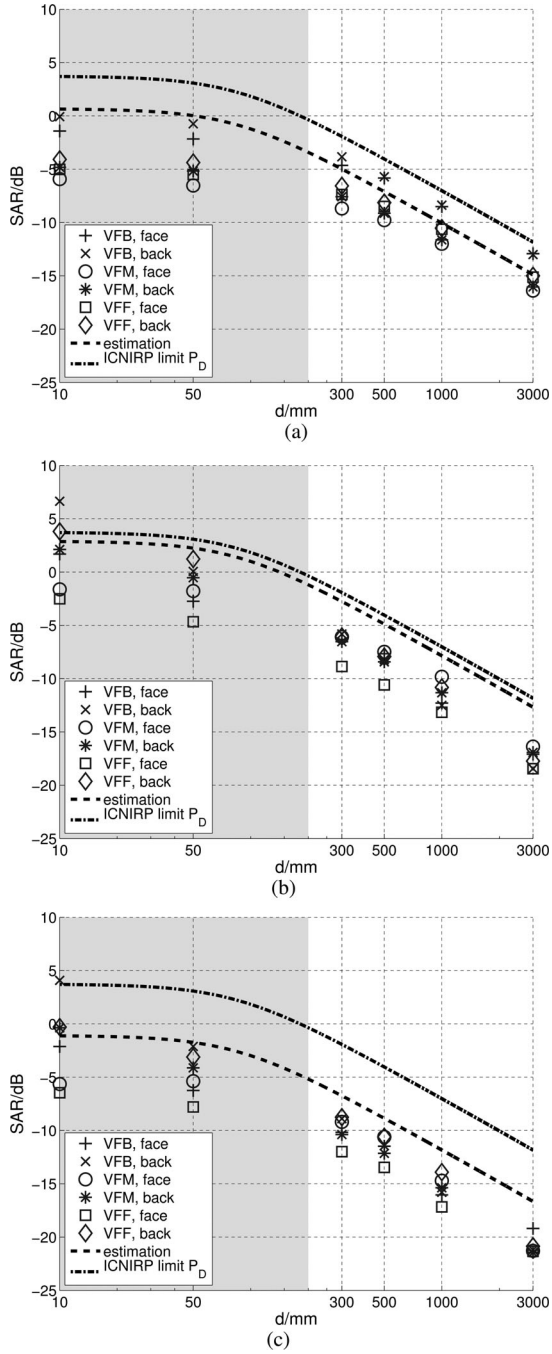

Fig. 9. Comparison of the simulation results of wbSAR and psSAR with the estimation formulas developed in Section IV and the ratio of (19) to the ICNIRP power density limit, for the antenna 900 MHz H65V7. The SAR is expressed as a ratio to the ICNIRP basic restrictions for a radiated power of 13.1 W. (a) wbSAR, (b) 1 g psSAR, and (c) 10 g psSAR.

1) twelve antennas (six frequencies: 300, 450, 900, 2100, 3500, and 5000 MHz);
2) six distances: 10, 50, 300, 500, 1000, and 3000 mm;
3) three human models: VFM, VFF, and VFB;
4) two exposure sides: front and back.

Only exposure from the front and the back of the model was simulated as it has already been shown to lead to the worst case wbSAR [3], [5], [7], [20]. The human models and the antennas are aligned center-to-center both horizontally and vertically.

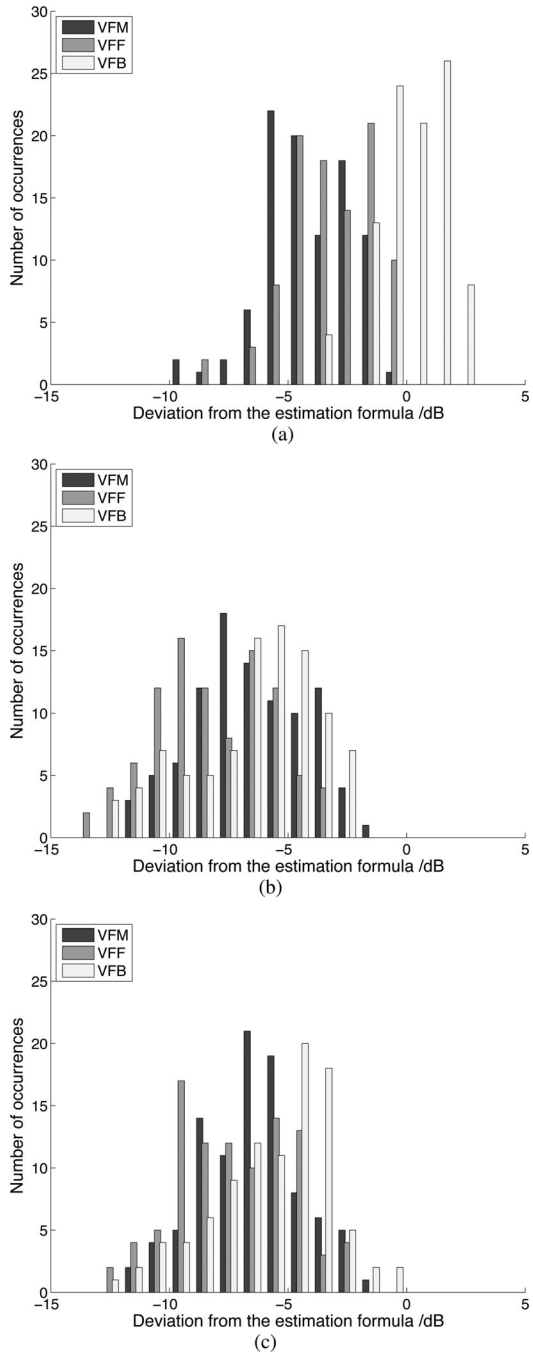

Fig. 10. Histograms of the deviation between the bulk simulation results of the three models (>200 mm) and the estimation formulas based on the 95th-percentile human body cuboid (simulation/estimation). (a) wbSAR, (b) 1 g psSAR, and (c) 10 g psSAR.

The comparison between the wbSAR and psSAR from the estimation formulas and from the simulations is presented in Fig. 9 for the antenna 900 MHz H65V7. The results are displayed as a ratio to the SAR limit (see Table IV), normalized such that the average power density 200 mm from the antenna computed with (19) is equal to the ICNIRP power density limit. For this antenna, this corresponds to a radiated power of 13.1 W. The curve of the ratio of the power density calculated from the antenna properties (19) to the ICNIRP power density limit is also shown.

It can be observed in Fig. 9 that the estimation formulas are conservative for the adult models at distances further than 200 mm, but not always for the VFB when considering the wbSAR. This is also the case for the 11 other antennas. At low frequencies, the ICNIRP power density limit is more conservative than the estimation formulas of the wbSAR and the psSAR (as can be seen in Fig. 9). For higher frequencies (not shown here), the ICNIRP power density limit is more conservative than the wbSAR estimation formula in almost every case and the 10 g psSAR estimation formula is only about 1 dB more conservative than the ICNIRP power density limit. However, the estimation of the 1 g psSAR is about 5 dB more conservative than the ICNIRP power density limit.

The results from Fig. 9, as well as the ones obtained for the 11 other antennas, are statistically analyzed to allow general observations and conclusions to be derived. Fig. 10 presents the deviation between the estimation formulas and the simulation results (>200 mm) for all the human models, sides of exposure, and antennas, where values lower than 0 dB represent configurations for which the formulas give a conservative estimation of the SAR. These histograms show that the estimation formulas for the wbSAR are more conservative than the results of the bulk simulations using the adult models, VFM and VFF, for all the simulation configurations (for distances higher than 200 mm). However, the estimation formulas for the wbSAR do not constitute a conservative approximation of the absorption in the VFB as only adults are taken into account in the statistical analysis leading to the 95th-percentile human. For the 1 g and 10 g psSAR, governed by the shape of the body rather that of its cross section, the results of the VFB are distributed similarly to the results from the adult models, and the estimation formulas are conservative for all the models and configurations (>200 mm).

VI. Discussion and Conclusion

The developed estimation formulas are based on the identified absorption mechanisms derived from physical considerations combined with plane-wave simulations of anatomical human bodies. They estimate the 95th-percentile wbSAR and psSAR values of adults (i.e., maintenance personal) in the vicinity of base-station antennas. The estimation formulas were validated with extensive simulations.

The validation by numerical means also demonstrates that the approximation is not always conservative for children. However, the available data do not allow determination of the uncertainty of the approximation with respect to the 95th-percentile exposure due to missing worst case anatomical/generic models. Nevertheless, confidence is high due to the step-by-step approximation with uncertainty analysis. The comparison with the simulated configurations provides no indication of a strong overestimation or underestimation of the 95th-percentile exposure. However, the estimation formulas only consider standing models, whereas a different posture could increase the psSAR.

In the reactive near-field region, estimation formulas as well as full-wave simulations have been found to be problematic in estimating human exposure due to the strong dependence of the localized absorption on the human anatomy. Furthermore,

the effects of reflections of the human body on the antenna impedance, the feeding network in particular and possibly the power amplifier, are not predictable with state-of-the-art simulation tools without detailed knowledge of the antenna feed system and its RF power source. Thus, at close antenna-body distances of less than 200 mm, SAR measurements are strongly recommended for demonstrating compliance. The selection of the most appropriate phantom needs to be investigated in future work.

ACKNOWLEDGMENT

The authors would like to thank Dr. A. Faraone for his input regarding antenna radiated power density, Dr. A. Hadjem and Dr. M.-F. Wong for their work on the antenna models, and L.-R. Harris for his contribution at Hokkaido University.

REFERENCES

[1] ICNIRP, "Guidelines for limiting exposure to time-varying electric, magnetic, and electromagnetic fields (up to 300 GHz)," *Health Phys.*, vol. 74, no. 4, pp. 494–522, 1998.

[2] IEEE SCC28, *IEEE Standard for Safety Levels with Respect to Human Exposure to Radio-Frequency Electromagnetic Fields, 3 kHz to 300 GHz*. International Committee on Electromagnetic Safety, The Institute of Electrical and Electronics Engineers, Inc., 3 Park Avenue, New York, NY 10016-5997, USA: IEEE Standards Department, IEEE C95.1-1991, 1991.

[3] M. C. Gosselin, A. Christ, S. Kühn, and N. Kuster, "Dependence of the occupational exposure to mobile phone base station on the properties of the antenna and the human body," *IEEE Trans. Electromagn. Compat.*, vol. 51, no. 2, pp. 227–235, May 2009.

[4] F. Lacroux, E. Conil, A. C. Carrasco, A. Gati, M.-F. Wong, and J. Wiart, "Specific absorption rate assessment near a base-station antenna (2140 MHz): Some key points," *Ann. Telecommun.*, vol. 63, no. 1–2, pp. 55–64, Feb. 2008.

[5] J. Cooper, B. Marx, J. Buhl, and V. Hombach, "Determination of safety distance limits for a human near a cellular base station antenna, adopting the IEEE Standard or ICNIRP Guidelines," *Bioelectromagnetics*, vol. 23, no. 6, pp. 429–443, 2002.

[6] W. Joseph and L. Martens, "Safety factor for determination of occupational electromagnetic exposure in phantom model," *Electron. Lett.*, vol. 39, no. 23, pp. 1663–4, Nov. 2003.

[7] S. Kühn, W. Jennings, A. Christ, and N. Kuster, "Assessment of induced radio-frequency electromagnetic fields in various anatomical human body models," *Phys. Med. Biol.*, vol. 54, no. 4, pp. 875–890, 2009.

[8] J. F. Bakker, M. M. Paulides, A. Christ, N. Kuster, and G. C. van Rhoon, "Assessment of induced SAR in children exposed to electromagnetic plane waves between 10 MHz and 5.6 GHz," *Phys. Med. Biol.*, vol. 55, no. 11, pp. 3115–3130, 2010.

[9] B. Thors, M. Strydom, B. Hansson, F. Meyer, K. Kärkkäinen, P. Zollman, S. Ilvonen, and C. Tornevik, "On the estimation of SAR and compliance distance related to RF exposure from mobile communication base station antennas," *IEEE Trans. Electromagn. Compat.*, vol. 50, no. 4, pp. 837–848, Nov. 2008.

[10] A. Christ, W. Kainz, E. G. Hahn, K. Honegger, M. Zefferer, E. Neufeld, W. Rascher, R. Janka, W. Bautz, J. Chen, B. Kiefer, P. Schmitt, H.-P. Hollenbach, J. Shen, M. Oberle, D. Szczerba, A. Kam, J. W. Guag, and N. Kuster, "The virtual family—Development of surface-based anatomical models of two adults and two children for dosimetric simulations," *Phys. Med. Biol.*, vol. 55, no. 2, pp. N23–N38, 2010.

[11] S. Gabriel, R. W. Lau, and C. Gabriel, "The dielectric properties of biological tissues: III. Parametric models for the dielectric spectrum of tissues," *Phys. Med. Biol.*, vol. 41, no. 11, pp. 2271–2293, 1996.

[12] Diverse Populations Collaborative Group, "Weight-height relationships and body mass index: Some observations from the diverse populations collaboration," *Amer. J. Phys. Anthropol.*, vol. 128, no. 1, pp. 220–229, 2005.

[13] IEEE, *Recommended Practice for Measurements and Computations of Radio Frequency Electromagnetic Fields With Respect to Human Exposure to Such Fields, 100 kHz-300 GHz*. International Committee on Electromagnetic Safety, The Institute of Electrical and Electronics Engineers, Inc., 3 Park Avenue, New York, NY 10016-5997, USA, IEEE Standards Department, IEEE Standard C95.3, Dec. 2002.

[14] S. Benkler, N. Chavannes, and N. Kuster, "New powerful FDTD source based on huygens surface: Highly complex EM simulations performed on an ordinary PC," Presented at the 31th Annu. Meeting Bioelectromagn. Soc., Davos, Switzerland, Jun. 14–19, 2009.

[15] A. Hirata, N. Ito, O. Fujiwara, T. Nagaoka, and S. Watanabe, "Conservative estimation of whole-body-averaged SARs in infants with a homogeneous and simple-shaped phantom in the GHz region," *Phys. Med. Biol.*, vol. 53, no. 24, pp. 7215–7223, 2008.

[16] A. Hirata, S. Kodera, J. Wang, and O. Fujiwara, "Dominant factors influencing whole-body average SAR due to far-field exposure in whole-body resonance frequency and GHz regions," *Bioelectromagnetics*, vol. 28, no. 6, pp. 484–7, 2007.

[17] R. Cicchetti and A. Faraone, "Estimation of the peak power density in the vicinity of cellular and radio base station antennas," *IEEE Trans. Electromagn. Compat.*, vol. 46, no. 2, pp. 275–290, May 2004.

[18] D. DuBois and E. F. DuBois, "A formula to estimate the approximate surface area if height and weight be known," *Arch. Internal Med.*, vol. 17, pp. 863–871, 1916.

[19] IEC, *Human Exposure to Radio-Frequency Fields from Handheld and Body-Mounted Wireless Communication Devices - Human Models, Instrumentation, and Procedures, Part 2: Procedure to determine the Specific Absorption Rate (SAR) for mobile wireless communication devices used in close proximity to the human body (frequency range of 30 MHz to 6 GHz), Draft*. Geneva, Switzerland, International Electrotechnical Commission (IEC), IEC Technical Committee 106, IEC 62209-2 Ed.1, 2009.

[20] T. Uusitupa, I. Laakso, S. Ilvonen, and K. Nikoskinen, "SAR variation study from 300 to 5000 MHz for 15 voxel models including different postures," *Phys. Med. Biol.*, vol. 55, no. 4, pp. 1157–1176, 2010.

[21] M. Kanda, M. Douglas, E. Mendivil, M. Ballen, A. Gessner, and C.-K. Chou, "Faster determination of mass-averaged SAR from 2-d area scans," *IEEE Trans. Microw. Theory Tech.*, vol. 52, no. 8, pp. 2013–2020, Aug. 2004.

[22] IEEE, *Recommended Practice for Determining the Spatial-Peak Specific Absorption Rate (SAR) in the Human Body due to Wireless Communications Devices: Measurement Techniques*, 445 Hoes Lane, P.O. Box 1331, Piscataway, NJ 08855-1331, USA, IEEE 1528/D1.2, Apr. 2003.

[23] A. Drossos, V. Santomaa, and N. Kuster, "The dependence of electromagnetic energy absorption upon human head tissue composition in the frequency range of 300–3000 MHz," *IEEE Trans. Microw. Theory Tech.*, vol. 48, no. 11, pp. 1988–1995, Nov. 2000.

[24] A. Christ, T. Samaras, A. Klingenböck, and N. Kuster, "Characterization of the electromagnetic near-field absorption in layered biological tissue in the frequency range from 30 MHz to 6000 MHz," *Phys. Med. Biol.*, vol. 51, no. 19, pp. 4951–4965, 2006.

[25] K. Meier, V. Hombach, R. Kästle, R. Y.-S. Tay, and N. Kuster, "The dependence of EM energy absorption upon human head modeling at 1800 MHz," *IEEE Trans. Microw. Theory Tech.*, vol. 45, no. 11, pp. 2058–2062, Nov. 1997.

[26] A. Christ, A. Klingenböck, T. Samaras, C. Goiceanu, and N. Kuster, "The dependence of electromagnetic far-field absorption on body tissue composition in the frequency range from 300 MHz to 6 GHz," *IEEE Trans. Microw. Theory Tech.*, vol. 54, no. 5, pp. 2188–2195, May 2006.

[27] A. Faraone, R. Y.-S. Tay, K. H. Joyner, and Q. Balzano, "Estimation of the average power density in the vicinity of cellular base-station collinear array antennas," *IEEE Trans. Veh. Technol.*, vol. 49, no. 3, pp. 984–996, May 2000.

[28] *FCC*, *Evaluating Compliance with FCC Guidelines for Human Exposure to Radio-Frequency Electromagnetic Fields, Supplement C to OET Bulletin 65*, Washington, DC 20554, Jun. 2001.

[29] IEC, *Human Exposure to Radio-Frequency Fields from Handheld and Body-Mounted Wireless Communication Devices - Human Models, Instrumentation, and Procedures, Part 2: Procedure to Determine the Specific Absorption Rate (SAR) for mobile wireless communication devices used in close proximity to the human body (frequency range of 30 MHz to 6 GHz), Draft*. Geneva, Switzerland: International Electrotechnical Commission (IEC), IEC Technical Committee 106, IEC 62209 Part 2, 2007.

[30] G. Vermeeren, M.-C. Gosselin, W. Joseph, S. Kühn, V. Kellerman, A. Hadjem, A. Gati, J. Wiart, F. Meyer, N. Kuster, and L. Martens, "Influence of the reflective environment on the absorption of a human male exposed to representative base-station antennas from 300 MHz to 5 GHz," *Phys. Med. Biol.*, vol. 55, no. 18, pp. 5541–5555, 2010.

Marie-Christine Gosselin was born in Sherbrooke, QC, Canada, in 1981. She received the B.Sc. and M.Sc. degrees in physics from the Université de Sherbrooke, Sherbrooke, in 2003 and 2006, respectively.

She joined the Foundation for Research on Information Technologies in Society, IT'IS Foundation, Switzerland, in January 2007, where she is engaged in various projects involving compliance to safety limits of human models exposed to mobile phones or base-station antennas. Her current research interests include the numerical assessment of the interaction mechanisms between electromagnetic fields and biological tissues.

Günter Vermeeren was born in Zottegem, Belgium, on March 9, 1976. He received the M.Sc. degree in industrial engineering from the KAHO Sint-Lieven, Ghent, Belgium, in July 1998 and also in electrical engineering from Ghent University, Ghent, in July 2001.

From September 2001 to September 2002, he was with the Research and Development Department of the Network Integrator Telindus, Leuven, Belgium. Since September 2002, he has been a Research Engineer in the WiCa group of Prof. L. Martens, where he is involved in several projects in the field of RF dosimetry, electromagnetic exposure, and on-body propagation. His current research interests include numerical modeling as well as measurements of electromagnetic fields in the proximity of humans.

Sven Kühn received the Dipl.Ing. (M.Sc.) degree in information and communication technologies from the Chemnitz University of Technology, Chemnitz, Saxony, Germany, and the Ph.D. (Dr. Sc.) degree in electrical engineering from Integrated Systems Laboratory (IIS), Swiss Federal Institute of Technology, ETH Zurich, Zurich, Switzerland, in 2004 and 2009, respectively.

In 2004, he joined the Foundation for Research on Information Technologies in Society (IT'IS), Switzerland, where he was involved in research on numerical and experimental methods for the assessment of human exposure to electromagnetic fields. He currently holds positions as a Project Leader for Experimental Dosimetry at the IT'IS Foundation, as a Head of Sensor Technologies at Schmid and Partner Engineering, AG, Zurich, and as a Postdoctoral Fellow at the IIS, ETH Zurich, and is a cofounder of Zurich Med Tech, Zurich. His main research interests include experimental and numerical dosimetry in bioelectromagnetics, near-field sensor, RF circuit, and antenna design, as well as biomedical applications thereof. Dr. Kühn is the recipient of the medal of the ETH Zurich as well as the award and a Research Grant of the Hans-Eggenberger Foundation for the Ph.D. thesis.

Valpré Kellerman was born in Pretoria, South Africa, in 1979. She received the B.Sc. Eng. degree and the M.Sc. Eng. (*cum laude*) degree both from Stellenbosch University, Stellenbosch, Western Cape, South Africa, in 2001 and 2004, respectively.

From 2005 to 2009, she was with EM Software and Systems (EMSS)-SA and EMSS-Consulting, Stellenbosch, where she was involved in various commercial and research projects on compliance of human models to safety standards, when exposed to electromagnetic radiation at various frequencies. She is currently self-employed with a lively interest in bioelectromagnetics.

Stefan Benkler was born in Bern, Switzerland, in 1974. He received the B.S. degree in microengineering from the University of Applied Sciences, Biel, Switzerland, in 1997, the M.S. degree in computational science and engineering from the Swiss Federal Institute of Technology, ETH Zurich, Zurich, Switzerland, in 2002, and the Ph.D. degree from the Laboratory for Integrated Systems (IIS), ETH Zurich, in 2006, focused mainly on developments and efficient implementations of subcell models to enhance real-world electromagnetic finite-difference time-domain (FDTD) simulations.

In 2002, he joined the Foundation for Research on Information Technologies in Society (IT'IS), ETH Zurich, concentrating on improving the conventional FDTD scheme with respect to effectiveness and application range. Since January 2007, he has been with the Schmid and Partner Engineering AG as a Software Developer of EM simulation platform SEMCAD X (numerical part). In the beginning, he concentrated on the development of a new low-frequency kernel. Meanwhile, he coordinates all research and development activities of the numerical solvers aside from his own implementation tasks. His main research interests include applied mathematics in general and time domain methods in particular.

Tero M. I. Uusitupa was born in Turku, Finland, in 1971. He received the M.Sc. and D.Sc. degrees from the Helsinki University of Technology, Espoo, Finland, in 1997 and 2004, respectively, both in electrical engineering.

Since 1995, he has been at the Department of Electrical and Communications Engineering of the Helsinki University of Technology (now: Aalto University, School of Science and Technology). Among teaching activities, his research has been in modeling of RF/microwave filters, waveguides, corrugated structures, and photonic-crystal components. In recent years, he has focused on parallel finite-difference time-domain (FDTD) modeling in dosimetry and background work for standardization of SAR assessment protocols. His current research interests include FDTD modeling of wireless body area networks.

Wout Joseph (M'05) was born in Ostend, Belgium, on October 21, 1977. He received the M.Sc. degree in electrical engineering from Ghent University, Ghent, Belgium, in July 2000, and the Ph.D. degree in March 2005 from the same university. His Ph.D. research dealt with measuring and modeling of electromagnetic fields around base stations for mobile communications related to the health effects of the exposure to electromagnetic radiation.

From September 2000 to March 2005, he was a Research Assistant in the Department of Information Technology (INTEC), Ghent University. During this period, his scientific work was focused on electromagnetic exposure assessment.

Since April 2005, he has been a Postdoctoral Researcher for IBBT-Ugent/INTEC (Interdisciplinary Institute for BroadBand Technology). Since October 2007, he has been a Postdoctoral Fellow of the FWO-V (Research Foundation—Flanders). Since October 2009, he has been a Professor in the domain of "Experimental Characterization of Wireless Communication Systems." His professional interests include electromagnetic field exposure assessment, propagation for wireless communication systems, antennas, and calibration. Furthermore, he specializes in wireless performance analysis and quality of experience.

Azeddine Gati (S'97–M'00) received the Engineer degree in telecommunication and signal processing in 1996, the M.Sc. degree from the University of Rennes, Rennes, France, and the Ph.D. degree from the University of Pierre and Marie Curie (Paris VI), Paris, France, in 2000.

From 1997 to 2001, he was engaged in studying circuit optimization and electromagnetic computational methods. Since 2001, he has been at Orange Labs, France Telecom, Issy les Moulineaux, France, where he is involved in research in the fields of applied electromagnetic for telecommunications systems. He is also involved in research on human interaction with radio waves. Since 2007, he has been leading research projects on sustainable development, including interactions of waves with human bodies, body area networks, wireless network planning tools, and energy in information, communication technology and service solutions.

Dr. Gati is a member of the Union Radio-Scientifique Internationale (URSI), France.

Joe Wiart received the Engineer degree from the Ecole Nationale Supérieure des Telecommunication (ENST), Paris, France, in 1992 and the Ph.D. degree in physics from the ENST and P&M Curie University, Paris, France, in 1995. He has been with Orange Labs since 1992 when he joined the Research Center of France Telecom, Issy les Moulineaux, France. Since 1994, he has been working on the interaction of radio waves with the human body and is heading of the Orange labs R&D unit WAVE. Since 2008, he has been the head of the Whist Lab, common laboratory of Orange Labs and Institut Telecom. He is the Chairperson of Union Radio-Scientifique Internationale (URSI) France. He is the French Representative in COST BM0704 and is Chairing the CENELEC TC 211 Working Group in charge of mobile and base station standard. He has published more than 50 papers in peer review journal. His research interests include electromagnetic compatibility, bioelectromagnetics, antenna measurements, computational electromagnetics, and statistics.

Dr. Wiart has been a Fellow of the Société des électriciens et des électroniciens (SEE) since 2008.

Frans J. C. Meyer received the B.Eng. degree in electronic engineering in 1988, the M.Eng. (*cum laude*) degree in 1991, and the Ph.D. degree in numerical techniques in electromagnetic engineering, in 1994, all from the University of Stellenbosch, Stellenbosch, Western Cape, South Africa.

He is the cofounder of EM Software and Systems (EMSS), a company specializing in the development of commercial software products for the electromagnetic simulations market, including the well-established FEKO suite of software. Since 1995, when EMSS was founded, he has been involved in bioelectromagnetic research and consulting work: first as a Principle Researcher and later as a Head of a small research group. The research group focused on human exposure to mobile phones and later on human exposure to base-station antennas. More recently, he and EMSS are working on mobile network compliance to international safety standards, which involves the development of numerical compliance software, field measurement projects, and training for RF workers.

Dr. Meyer has been a member of the Bioelectromagnetics Society (BEMS) for the past 11 years.

Luc Martens (M'92) was born in Ghent, Belgium, on May 14, 1963. He received the M.Sc. degree in electrical engineering from Ghent University, Ghent, in July 1986, and the Ph.D. degree from the same university in 1990. His Ph.D. research dealt with electromagnetic and thermal modeling and with the development of measurement systems for that application.

From September 1986 to December 1990, he was a Research Assistant at the Department of Information Technology (INTEC), Ghent University, where his scientific work was focused on the physical aspects of hyperthermic cancer therapy. Since January 1991, he has been a Permanent Staff Member of the Interuniversity MicroElectronics Centre (IMEC), Ghent, and is responsible for the research on experimental characterization of the physical layer of telecommunication systems at INTEC. His group also studies topics related to the health effects of wireless communication devices. Since April 1993, he has been a Professor of Electrical Applications of Electromagnetism at Ghent University.

Toshio Nojima received the B.E. degree in electrical engineering from Saitama University, Saitama, Japan, in 1972 and the M.E. and Ph.D. degrees from Hokkaido University, Sapporo, Japan, in 1974 and 1988, respectively, both in electronic engineering.

From 1974 to 1992, he was with Nippon Telegraph and Telephone (NTT) Communications Laboratories, where he was engaged in the development of microwave relay systems. From 1992 to 2001, he was with NTT DoCoMo, Inc., where he was a Senior Executive Research Engineer and involved in research on the radio safety issues of RF exposures as well as mobile communication technologies. Since January 2002, he has been a Professor at the Graduate School of Information Science and Technology, Hokkaido University.

Dr. Nojima is a member of the Bioelectromagnetics Society (BEMS) and the Institute of Electronics, Information, and Communication Engineers of Japan (IEICE).

Takashi Hikage received the B.E., M.E., and Ph.D. degrees from Hokkaido University, Sapporo, Japan, in 1997, 1999, and 2002, respectively, all in electronics and information engineering.

From 1999 to 2003, he was with the Graduate School of Engineering, Hokkaido University. He is currently an Assistant Professor of the Graduate School of Information Science and Technology, Hokkaido University.

Dr. Hikage is a member of the Institute of Electronics, Information, and Communication Engineers of Japan (IEICE).

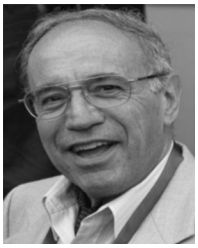

Quirino Balzano (LF'05) received the Doctor's degree in electronics engineering from the University of Rome, La Sapienza, Rome, Italy, in December 1965.

In 1966, he was at FIAT, SpA, Turin, Italy. From 1967 to 1974, he was with the Missile Systems Division of Raytheon Company, Bedford, MA. He was involved in the research, design, and development of planar and conformal phased arrays for the Patriot and other missile systems. In 1974, he joined the Motorola, Inc., Portable Products Division, Plantation, FL, where he achieved the position of Corporate Vice President and Director of the Portable Products Research Laboratories. He retired from Motorola in February 2001. Since August 2002, he has been a Senior Staff Researcher in the Electrical and Computer Engineering (ECE) Department, University of Maryland, College Park, MD. He teaches a course on antennas at American, European, and Asian Universities. He has 31 patents in antenna and IC technology and has authored or coauthored 100 publications.

Dr. Balzano received the IEEE Vehicular Technology Society Best Paper of the year Award in 1978 and 1982. He is the past (2005) Chair of Commission A (Measurements) of the International Union of Radio Science (URSI).

Andreas Christ was born in Offenbach, Germany, in 1968. He received the Dipl.Ing. degree in electrical engineering from the Technical University Darmstadt, Darmstadt, Germany, in 1996. In 1997, he joined Niels Kuster's Research Group at the Swiss Federal Institute of Technology, ETH Zurich, where he received the Ph.D. degree in 2003.

Since 2003, he has been with the Foundation for Research on Information Technologies in Society, (IT'IS) Foundation, where he is leading the Numerical Dosimetry Group. He is involved in the assessment of interaction mechanisms of electromagnetic fields and biological tissue. He actively participates in the development of numerical and experimental techniques to evaluate the safety of magnetic resonance imaging for patients with medical implants within the joint working group of ISO/TC 150/SC 6/JWG2 and IEC SC 62B. His further research interests include computational electrodynamics with the finite-difference time-domain method, the development of anatomical models for dosimetric simulations, and the numerical modeling of medical devices.

Dr. Christ is member of the European BioElectromagnetics Association (EBEA), the Bioelectromagnetics Society (BEMS), and the IEEE Standards Association, where he chairs the Working Group 1 of Technical Committee 34: Wireless Handset SAR Certification, Subcommittee 2: Computational Techniques.

Niels Kuster (F'11) received the M.S. and Ph.D. degrees from the Swiss Federal Institute of Technology, ETH Zurich (ETHZ), Zurich, both in electrical engineering.

Between 1993 and 1999, he was an Assistant Professor at the Department of Electrical Engineering, ETHZ. He was awarded Professor at the Department of Information Technology and Electrical Engineering, ETHZ, in 2001. From 1999 until now, he has served as the Founding Director of the Foundation for Research on Information Technologies in Society (IT'IS), Switzerland. In 2010, he initiated the sister institute IT'IS USA, a nonprofit research unit incorporated in Maryland, of which he is currently the President. During his career, he has held invited Professorships at the Electromagnetics Laboratory of Motorola, Inc., FL, and at the Metropolitan University, Tokyo, Japan, in 1998. He also founded several spin-off companies Schmid & Partner Engineering AG, MaxWave AG, NFT Holding AG, Zurich MedTech AG and advises other companies as board member such as IMRICOR, Inc., TheraBionic LLC, etc. He has published more than 600 publications (books, journals, and proceedings) on measurement techniques, computational electromagnetics, dosimetry, exposure assessments, and bioexperiments. His primary research interests include safe and beneficial applications of electromagnetic fields in health and information technologies. He is particularly interested in measurement technology; computational electrodynamics for the evaluation of close near fields in complex environments (e.g., handheld or body-mounted transceivers, residential/work environments, etc.); safe and reliable wireless communication links within the body or between implanted devices and exterior equipment for biometric applications; development of exposure setups and quality control for bioexperiments to evaluate interaction mechanisms, therapeutic effects and potential health risks; exposure assessments; EM safety of medical devices; medical diagnostic and therapeutic applications of EM, in particular EM cancer treatment modalities; and virtual patient applications. He is currently building up a new research team in computational life science in biology.

Dr. Kuster is a member of several standardization bodies and acts as a consultant to government agencies around the globe on the safety of mobile communications. He was a board member of various scientific societies and boards, was Bioelectromagnetics Society (BEMS) president in 2008–2009. He is delegate of the Swiss Academy of Science and is currently an Associate Editor of the IEEE Transactions on Electromagnetic Compatibility.